(4)

OFFICE OF NAVAL RESEARCH

Contract N00014-86-K-0043

TECHNICAL REPORT No. 73

Light Scattering by a Phase Conjugator in the Four-Wave Mixing Configuration

by

Henk F. Arnoldus and Thomas F. George

Prepared for Publication

in

Journal of Modern Optics

Departments of Chemistry and Physics
State University of New York at Buffalo
Buffalo, New York 14260

June 1988

UNCLASSIFIED
SECURITY CLASSIFICATION OF THIS PAGE

REPORT DOCUMENTATION PAGE

Form Approved OMB No. 0704-0188

1a. REPORT SECURITY CLASSIFICATION: Unclassified	1b. RESTRICTIVE MARKINGS
2a. SECURITY CLASSIFICATION AUTHORITY	3. DISTRIBUTION/AVAILABILITY OF REPORT: Approved for public release; distribution unlimited
2b. DECLASSIFICATION/DOWNGRADING SCHEDULE	
4. PERFORMING ORGANIZATION REPORT NUMBER(S): UBUFFALO/DC/88/TR-73	5. MONITORING ORGANIZATION REPORT NUMBER(S)
6a. NAME OF PERFORMING ORGANIZATION: Depts. Chemistry & Physics, State University of New York; 6b. OFFICE SYMBOL (If applicable)	7a. NAME OF MONITORING ORGANIZATION
6c. ADDRESS (City, State, and ZIP Code): Fronczak Hall, Amherst Campus, Buffalo, New York 14260	7b. ADDRESS (City, State, and ZIP Code): Chemistry Program, 800 N. Quincy Street, Arlington, Virginia 22217
8a. NAME OF FUNDING/SPONSORING ORGANIZATION: Office of Naval Research; 8b. OFFICE SYMBOL (If applicable)	9. PROCUREMENT INSTRUMENT IDENTIFICATION NUMBER: Contract N00014-86-K-0043
8c. ADDRESS (City, State, and ZIP Code): Chemistry Program, 800 N. Quincy Street, Arlington, Virginia 22217	10. SOURCE OF FUNDING NUMBERS: PROGRAM ELEMENT NO. / PROJECT NO. / TASK NO. / WORK UNIT ACCESSION NO.

11. TITLE (Include Security Classification)

Light Scattering by a Phase Conjugator in the Four-Wave Mixing Configuration

12. PERSONAL AUTHOR(S): Henk F. Arnoldus and Thomas F. George

13a. TYPE OF REPORT	13b. TIME COVERED FROM _____ TO _____	14. DATE OF REPORT (Year, Month, Day)	15. PAGE COUNT
		June 1988	45

16. SUPPLEMENTARY NOTATION

Prepared for publication in Journal of Modern Optics

17. COSATI CODES			18. SUBJECT TERMS (Continue on reverse if necessary and identify by block number)
FIELD	GROUP	SUB-GROUP	LIGHT SCATTERING, PHASE CONJUGATOR, FOUR-WAVE MIXING, PHASE-MATCHING RESONANCES, FINITE INCIDENCE ANGLE, SPECTROSCOPIC APPLICATIONS

19. ABSTRACT (Continue on reverse if necessary and identify by block number)

Reflection of travelling and evanescent plane waves by a four-wave mixing phase conjugator is studied in detail. No restrictions are imposed on the nonlinear interaction strength, the angle of incidence or the frequency mismatch between the pump beams and the incoming waves. We only assume that the incident field is weak compared to the pump fields, which justifies a classical-field description of the pumps. The wave vectors, amplitudes and phases for the various waves are evaluated, without the slowly-varying amplitude approximation. Familiar phase-matching resonances for certain values of the interaction length are recovered, and in addition strong resonances are found if the angle of incidence is finite, and the incident light is not in perfect resonance with the pumps. The latter resonances appear at the transitions from a travelling to an evanescent wave. The significance of finite angles of incidence and evanescent waves for spectroscopic applications is pointed out.

20. DISTRIBUTION/AVAILABILITY OF ABSTRACT	21. ABSTRACT SECURITY CLASSIFICATION
☒ UNCLASSIFIED/UNLIMITED ☒ SAME AS RPT. ☐ DTIC USERS	Unclassified
22a. NAME OF RESPONSIBLE INDIVIDUAL: Dr. David L. Nelson	22b. TELEPHONE (Include Area Code): (202) 696-4410; 22c. OFFICE SYMBOL

DD Form 1473, JUN 86 — Previous editions are obsolete.

SECURITY CLASSIFICATION OF THIS PAGE
UNCLASSIFIED

Journal of Modern Optics, in press

LIGHT SCATTERING BY A PHASE CONJUGATOR IN THE FOUR-WAVE MIXING CONFIGURATION

Henk F. Arnoldus and Thomas F. George
Department of Physics
239 Fronczak Hall
State University of New York at Buffalo
Buffalo, New York 14260, USA

Abstract

Reflection of travelling and evanescent plane waves by a four-wave mixing phase conjugator is studied in detail. No restrictions are imposed on the nonlinear interaction strength, the angle of incidence or the frequency mismatch between the pump beams and the incoming waves. We only assume that the incident field is weak compared to the pump fields, which justifies a classical-field description of the pumps. The wave vectors, amplitudes and phases for the various waves are evaluated, without the slowly-varying amplitude approximation. Familiar phase-matching resonances for certain values of the interaction length are recovered, and in addition strong resonances are found if the angle of incidence is finite, and the incident light is not in perfect resonance with the pumps. The latter resonances appear at the transitions from a travelling to an evanescent wave. The significance of finite angles of incidence and evanescent waves for spectroscopic applications is pointed out.

PACS: 03.50.De, 41.10.Hv, 42.65.Hw

1. Introduction

Among the many ways [1-3] of generating a phase-conjugated signal with respect to a reference signal, the technique of four-wave mixing is the most promising from an experimental point of view [4-9]. A nonlinear crystal (like $BaTiO_3$) or liquid (typically CS_2) is irradiated by two counterpropagating strong laser beams (the pumps) with intensity I. A third incident (weak) field then couples to the pump fields through the third-order susceptibility $\chi^{(3)}$, and the result is an electric polarization of the medium, which is proportional to $\chi^{(3)}I$ and the electric field component of the weak field. This induced polarization then emits radiation which propagates out of the crystal. Under certain conditions this generated fourth wave is the phaase-conjugated, or time-reversed, replica of the incident field. Production of phase-conjugated radiation is of great practical importance in optical engineering, because it provides a method for correction of wavefront distortions.

In most applications the weak field is a nearly-monochromatic plane wave with well-defined polarization, the angle of incidence on the crystal is almost zero (usually a few degrees), and the coupling constant $\gamma \propto \chi^{(3)}I$ is very small. For this configuration the generation of phase-conjugated waves is well-understood [10-19]. There are, however, conceivable applications in which these conditions do not hold. It has been predicted, for instance, that the lifetime of an atom in the neighborhood of a phase conjugator (PC) is infinite, as a result of the fact that an ideal PC focusses the emitted fluorescence exactly back on the atom [20,21]. Consequently, the spectroscopic linewidth of the atomic transition under consideration would be zero, which can have a great impact on frequency standards. These predictions were derived under the assumption of perfect phase conjugation. Since phase conjugation is equivalent to time reversal, it is obvious that ideal PC's cannot exist (violates

causality). Nevertheless it can be anticipated that realistic PC's can possibly be utilized to manipulate linewidths over a large range (in contrast to the situation of atoms near a metal surface, where the change in lifetime is at best a factor of two).

Emitted dipole radiation (fluorescence) by an atom in the vicinity of a PC has plane-wave components, which are incident on the surface under every angle of incidence. Besides that, a dipole field has evanescent components (exponentially-decaying waves) [22], and the radiation is not monochromatic. Furthermore, for contemporary high-power lasers the interaction parameter $\gamma \propto I$ is not necessarily small. In this paper we present a general treatment of the scattering of travelling and evanescent waves by a four-wave mixing PC, without restrictions on the interaction strength, frequency, polarization or angle of incidence.

2. The model

A nonlinear transparent crystal ($\chi^{(3)} \neq 0$, $\chi^{(i\neq 3)} = 0$) occupies the region $0 > z > -\Delta$, $\Delta > 0$, in an xyz Cartesian coordinate frame, and the regions $z > 0$ and $z < -\Delta$ are empty space. Two counter-propagating pump beams with intensity I and frequency $\bar{\omega}$ (called the setting frequency of the PC) illuminate the medium. Then the complex-valued coupling parameter is given by $\gamma \propto \chi^{(3)} I$. We shall assume that I is constant (no depletion of pumps) and that $\chi^{(3)}$ is frequency independent. This means that the incident probe field must have a bandwidth around $\bar{\omega}$ which is smaller than the frequency width of $\chi^{(3)}$. In this fashion we can avoid complicated notations, but it is straightforward to retain the frequency dependence of γ if necessary [23]. Furthermore, we assume that the tensorial nature of $\chi^{(3)}$ is irrelevant, which can always be managed by a proper choice of geometry.

The radiation field shall be represented by its electric and magnetic components $\underline{E}(\underline{r},t)$ and $\underline{B}(\underline{r},t)$, respectively, and charges and currents by a polarization density $\underline{P}(\underline{r},t)$. It is advantageous to adopt a Fourier transform with respect to time,

$$\hat{\underline{E}}(\underline{r},\omega) = \int_{-\infty}^{\infty} dt\, e^{i\omega t}\, \underline{E}(\underline{r},t) \quad , \ \omega \text{ real}, \tag{2.1}$$

and since $\underline{E}(\underline{r},t)$ is real we have

$$\hat{\underline{E}}(\underline{r},-\omega) = \hat{\underline{E}}(\underline{r},\omega)^* \quad . \tag{2.2}$$

Similar notations apply to $\underline{B}(\underline{r},t)$ and $\underline{P}(\underline{r},t)$. In the Fourier domain Maxwell's equations read

$$\begin{aligned} &\nabla\cdot(\hat{\underline{E}} + \hat{\underline{P}}/\epsilon_0) = 0 \quad , \quad \nabla\cdot\hat{\underline{B}} = 0 \quad , \\ &\nabla \times \hat{\underline{E}} = i\omega\hat{\underline{B}} \quad , \quad \nabla \times \hat{\underline{B}} = \frac{-i\omega}{c^2}\,(\hat{\underline{E}} + \hat{\underline{P}}/\epsilon_0) \quad , \end{aligned} \tag{2.3}$$

which should hold for all $\underline{r}$ and ω.

In the regions $z > 0$ and $z < -\Delta$ the polarization density $\hat{\underline{P}}$ is zero. Inside the nonlinear medium the $\hat{\underline{P}}(\underline{r},\omega)$ is proportional to the electric field at a different frequency. Explicitly [24], this has the form

$$\underline{\hat{P}}(\underline{r},\omega) = \begin{cases} \epsilon_0 \gamma^* \, \underline{\hat{E}}(\underline{r},\omega-2\bar{\omega}) \quad , \quad \omega > 0 \quad , \\ \\ \epsilon_0 \gamma \, \underline{\hat{E}}(\underline{r},2\bar{\omega}+\omega) \quad , \quad \omega < 0 \quad , \end{cases} \tag{2.4}$$

where the field $\underline{\hat{E}}$ does not include the two pump fields. These are parametrically accounted for by $\gamma \propto I$. On the surfaces $z = 0$ and $z = -\Delta$, Maxwell's equations (2.3) imply the usual boundary conditions.

3. Dispersion relation

Before we can solve the scattering problem for travelling and evanescent waves by this PC, we have to establish the fundamental plane-wave solutions which are supported by the medium. To this end we first notice that the polarization density $\underline{\hat{P}}(\underline{r},\omega)$ from Eq. (2.4) couples positive and negative frequencies. If we denote by $\omega_1 \approx \bar{\omega} > 0$ a fixed positive frequency, then $\underline{\hat{P}}(\underline{r},\omega_1)$ is determined by the electric field component with frequency

$$\omega_2 = \omega_1 - 2\bar{\omega} \quad . \tag{3.1}$$

The polarization at this negative frequency $\omega_2 \approx -\bar{\omega}$ is then proportional to the electric field at $2\bar{\omega} + \omega_2 = \omega_1$, according to Eq. (2.4). Hence the nonlinear interaction couples positive and negative frequencies ω_1 and ω_2 in pairs. Consequently, for a fixed ω_1 Maxwell's equations (2.3) constitute essentially a set of eight equations, which have to be solved simultaneously.

The third Maxwell equation can be written as

$$\underline{\hat{B}}(\underline{r},\omega) = \frac{-i}{\omega} \nabla \times \underline{\hat{E}}(\underline{r},\omega) \quad , \tag{3.2}$$

and therefore $\hat{\underline{B}}$ is known as soon as we have found $\hat{\underline{E}}$, both for ω_1 and ω_2. Then, $\nabla\cdot\hat{\underline{B}} = 0$ is automatically satisfied. Furthermore, we notice that $\hat{\underline{P}}$ is proportional to $\hat{\underline{E}}$, although at a different frequency, and so the first Maxwell equation is certainly obeyed if

$$\nabla\cdot\hat{\underline{E}}(\underline{r},\omega) = 0 \quad , \tag{3.3}$$

for every ω. Next we substitute Eqs. (2.4) and (3.2) into the fourth Maxwell equation, which yields the set of coupled-wave equations

$$(\nabla^2 + (\frac{\omega_1}{c})^2)\ \hat{\underline{E}}(\underline{r},\omega_1) = -\gamma^*(\frac{\omega_1}{c})^2\ \hat{\underline{E}}(\underline{r},\omega_2) \quad , \tag{3.4}$$

$$(\nabla^2 + (\frac{\omega_2}{c})^2)\ \hat{\underline{E}}(\underline{r},\omega_2) = -\gamma(\frac{\omega_2}{c})^2\ \hat{\underline{E}}(\underline{r},\omega_1) \quad , \tag{3.5}$$

for the electric field. Equations (3.3)-(3.5) are the basic relations for a PC. The first one states that the fields are transverse, and (3.4) and (3.5) show that a wave with a positivie frequency ω_1 couples to a wave with a negative frequency ω_2, and vice versa. Therefore, a positive-frequency field generates a negative-frequency field, which is the essence of a phase conjugator.

As a plane-wave solution we try

$$\hat{\underline{E}}_a(\underline{r},\omega_1) = \underline{E}_a\ e^{i\underline{k}_a\cdot\underline{r}} \quad , \tag{3.6}$$

$$\hat{\underline{E}}_a(\underline{r},\omega_2) = \eta_a\underline{E}_a\ e^{i\underline{k}_a\cdot\underline{r}} \quad . \tag{3.7}$$

Then Eqs. (3.3) - (3.5) give

$$\underline{k}_a \cdot \underline{E}_a = 0 \quad , \tag{3.8}$$

$$k_a^2 = k^2(1 + \gamma^* \eta_a) = k^2 \rho^2 (1 + \gamma/\eta_a) \quad , \tag{3.9}$$

where we introduced the wave number

$$k = \omega_1/c \quad ,$$

and the dimensionless detuning parameter

$$\rho = 2\bar{\omega}/\omega_1 - 1 \quad . \tag{3.10}$$

Equation (3.8) states that plane waves in a PC are transverse, and the last equality in Eq. (3.9) gives an equation for the amplitude ratio η_a between the ω_2 and the ω_1 component. Because Eq. (3.9) is quadratic in η_a, it admits two solutions. For reasons which will become clear in due course, we choose the solution

$$\eta_a = \{\rho^2 - 1 - \delta((\rho^2-1)^2 + 4\gamma_0^2\rho^2)^{1/2}\}/2\gamma^* \quad , \tag{3.11}$$

with

$$\gamma = \gamma_0 e^{i\phi} \quad , \quad \gamma_0 > 0 \quad , \quad \phi \text{ real} \quad , \tag{3.12}$$

$$\delta = \mathrm{sgn}(\bar{\omega}-\omega_1) = \mathrm{sgn}(\rho-1) \quad . \tag{3.13}$$

The solution corresponding to the second root for η_a will be written as

$$\hat{\underset{\sim}{E}}_b(\underset{\sim}{r},\omega_1) = \eta_b \underset{\sim}{E}_b \, e^{i\underset{\sim}{k}_b\cdot\underset{\sim}{r}} \quad , \tag{3.14}$$

$$\hat{\underset{\sim}{E}}_b(\underset{\sim}{r},\omega_2) = \underset{\sim}{E}_b \, e^{i\underset{\sim}{k}_b\cdot\underset{\sim}{r}} \quad , \tag{3.15}$$

which obeys Maxwell's equations if

$$\underset{\sim}{k}_b\cdot\underset{\sim}{E}_b = 0 \quad , \tag{3.16}$$

$$k_b^2 = k^2\rho^2(1 + \gamma\eta_b) = k^2(1 + \gamma^*/\eta_b) \quad . \tag{3.17}$$

Of the two possible solutions for η_b we have to take

$$\eta_b = (1 - \rho^2 + \delta((\rho^2-1)^2 + 4\gamma_0^2\rho^2)^{1/2})/2\gamma\rho^2 \quad . \tag{3.18}$$

With this convention we have $\eta_a \to 0$, $\eta_b \to 0$ if $\gamma \to 0$, and the a and b solutions become (uncoupled) ω_1 and ω_2 waves, respectively, in this limit. For $\gamma \neq 0$ the parameters η_a and η_b determine the relative strengths of the coupled waves with the complementary frequency, which are excited by the four-wave mixing process. Furthermore, we notice that the coupled waves $\hat{\underset{\sim}{E}}_a(\underset{\sim}{r},\omega_1)$ and $\hat{\underset{\sim}{E}}_a(\underset{\sim}{r},\omega_2)$ have the same wave vector $\underset{\sim}{k}_a$, which implies a perfect phase matching between these two waves at different frequencies. The same holds for the b-solution.

Now we can substitute the expressions for η_a and η_b into Eqs. (3.9) and (3.17), which gives the wave numbers k_a and k_b (up to a minus sign). Notations can be simplified considerably by the introduction of the quantity

$$\epsilon = \tfrac{1}{2}(\rho^2+1-\delta((\rho^2-1)^2 + 4\gamma_0^2\rho^2)^{\frac{1}{2}}) \quad . \tag{3.19}$$

Then we find in terms of ϵ

$$k_a^2 = k^2\epsilon \quad , \quad k_b^2 = k^2(\rho^2+1-\epsilon) \quad , \tag{3.20}$$

$$\eta_a = (\epsilon-1)/\gamma^* \quad , \quad \eta_b = (1-\epsilon)/\gamma\rho^2 \quad . \tag{3.21}$$

If the medium would be an ordinary dielectric, we would also have $k_a^2 = k^2\epsilon$, but with ϵ as the dielectric constant. An important difference is that in Eq. (3.19) the ϵ depends explicitly on the frequency ω_1 through the parameter ρ. This frequency dependence is a genuine geometrical effect, as it follows from the mechanism of four-wave mixing (rather than from a frequency dependence of $\chi^{(3)}$, which we have suppressed). Therefore, Eq. (3.20) gives the fundamental relations for the two branches of the dispersion curve for a four-wave mixing PC. This universal dispersion relation is plotted in Fig. 1. We remark that ϵ, as defined in Eq. (3.19), is real (possibly negative). If the frequency dependence of $\chi^{(3)}$ would have been retained, then ϵ could also have an imaginary part. Furthermore, we notice that ϵ is discontinuous across the resonance $\omega_1 = \bar{\omega}$, or $\rho = 1$, due to the appearance of δ.

4. Incident field

A given external field illuminates the surface z = 0 of the PC. Since almost every field can be expanded in plane waves, and since Maxwell's equations for this PC are linear (even though the four-wave mixing process is not), it suffices to consider an incident field of the form

$$\underset{\sim}{\hat{E}}_{inc}(\underset{\sim}{r},\omega_1) = \underset{\sim}{E}_{inc}\, e^{i\underset{\sim}{k}\cdot\underset{\sim}{r}} \quad , \tag{4.1}$$

defined in the region z > 0. The corresponding $\underset{\sim}{\hat{B}}$ field follows from Eq. (3.2). In Eq. (4.1) the polarization and amplitude $\underset{\sim}{E}_{inc}$, and the wave vector $\underset{\sim}{k}$ are arbitrary, with the only restrictions

$$\underset{\sim}{k}\cdot\underset{\sim}{E}_{inc} = 0 \quad , \quad k^2 = \underset{\sim}{k}\cdot\underset{\sim}{k} = (\omega_1/c)^2 \quad , \tag{4.2}$$

according to Maxwell's equations in z > 0.

With the unit vector $\underset{\sim}{e}_z$ as the normal to the surface, we can decompose $\underset{\sim}{k}$ into its parallel and perpendicular components with respect to the xy-plane. We write

$$\underset{\sim}{k} = \underset{\sim}{k}_{\parallel} + k_z\underset{\sim}{e}_z \quad , \tag{4.3}$$

and similarly for any other vector quantity. Combining this with Eq. (4.2) gives

$$k_z^2 = k^2 - k_{\parallel}^2 \quad . \tag{4.4}$$

The quantity k^2 is a given positive number for a fixed ω_1, but the components $\underset{\sim}{k}_\parallel$ and $k_z\underset{\sim}{e}_z$ of $\underset{\sim}{k}$ can be anything, as long as restriction (4.4) is satisfied. For most practical cases it is sufficient to consider only real-valued vectors $\underset{\sim}{k}_\parallel$, and this will be assumed from now on. We shall regard the quantities $k = \omega_1/c > 0$ and $\underset{\sim}{k}_\parallel$ as given, but arbitrary. Then, the right-hand side of Eq. (4.4) is a given real number, and there are two possible solutions for k_z. Because the external field is generated by sources in the region $z > 0$, we have to choose the causal solution, which is

$$k_z = \begin{cases} -\sqrt{k^2 - k_\parallel^2}\,, & \text{if } k > k_\parallel\,, \\ -i\sqrt{k_\parallel^2 - k^2}\,, & \text{if } k < k_\parallel\,, \end{cases} \tag{4.5}$$

where $k_\parallel = \sqrt{\underset{\sim}{k}_\parallel \cdot \underset{\sim}{k}_\parallel} > 0$. For $k > k_\parallel$ the k_z is negative and real, corresponding to an incident travelling plane wave from the region $z > 0$. In the case $k < k_\parallel$, k_z is imaginary, and the root is chosen in such a way that the wave decays exponentially to zero in amplitude in the negative z-direction. This evanescent wave decays in the direction perpendicular to the surface, and travels along the surface in the $\underset{\sim}{k}_\parallel$-direction.

5. Fields

The incident field $\hat{\underset{\sim}{E}}_{inc}(\underset{\sim}{r},\omega_1)$ induces a nonlinear polarization in the medium, which in turn emits radiation according to the coupled-wave equations (3.4) and (3.5). This radiation travels out of the crystal and gives rise to reflected and transmitted waves by the layer. It will turn out that the fields

everywhere in space can be expressed in plane travelling or evanescent waves, depending on k and $k_{\parallel}$. Every wave α will therefore have a spatial dependence of $\underset{\sim}{E}_{\alpha}\exp(i\underset{\sim}{k}_{\alpha}\cdot\underset{\sim}{r})$. Transversality then requires

$$\underset{\sim}{k}_{\alpha}\cdot\underset{\sim}{E}_{\alpha} = 0 \quad , \tag{5.1}$$

for every wave. Since the waves must be matched across the planes $z = 0$ and $z = -\Delta$ with the aid of boundary conditions, which should hold for all $\underset{\sim}{r}$ in $z = 0$ and $z = -\Delta$, all wave vectors must have the same parallel component. Therefore, we have

$$\underset{\sim}{k}_{\alpha} = \underset{\sim}{k}_{\parallel} + k_{\alpha,z}\underset{\sim}{e}_{z} \quad , \tag{5.2}$$

and only $k_{\alpha,z}$ remains to be determined. On the other hand, the dispersion relations in vacuum and in the PC fix the value of $k_{\alpha}^2 = k_{\parallel}^2 + k_{\alpha,z}^2$. Consequently, the only freedom we have left is the choice of the sign of $k_{\alpha,z}$. In the regions $z > 0$ and $z < -\Delta$ this sign is determined by the requiremen that the waves must emanate from the PC, in the same way as we found the sign of k_z. For the fields inside the PC there is no <u>a priori</u> way to fix the signs of the z-components of the wave vectors, and therefore we have to retain all possible combinations. We shall only write down the expressions for the electric fields. Then, the magnetic fields can be found from Eq. (3.2).

5.1 <u>Region $z > 0$</u>

From the arguments above it follows that the most general plane-wave solution in the region $z > 0$ is given by

$$\underset{\sim}{\hat{E}}(\underset{\sim}{r},\omega_1) = \underset{\sim}{E}_{inc}\, e^{i\underset{\sim}{k}\cdot\underset{\sim}{r}} + \underset{\sim}{E}_{r}\, e^{i\underset{\sim}{k}_r\cdot\underset{\sim}{r}} \quad , \tag{5.3}$$

$$\underset{\sim}{\hat{E}}(\underset{\sim}{r},\omega_2) = \underset{\sim}{E}_{pc}\, e^{i\underset{\sim}{k}_{pc}\cdot\underset{\sim}{r}} \quad . \tag{5.4}$$

At frequency ω_1 there is only one other possible wave, which is the specularly-reflected r-wave with

$$k_r = k \quad , \quad k_{r,z} = -k_z \quad . \tag{5.5}$$

Although this field resembles the reflected wave by an ordinary dielectric, it is here entirely generated by the four-wave mixing process (we have set $\chi^{(1)} = 0$). At ω_2 we have the phase-conjugated pc-wave with

$$k_{pc} = -\omega_2/c > 0 \quad , \tag{5.6}$$

$$k_{pc,z}^2 = k_{pc}^2 - k_{\|}^2 = k^2\rho^2 - k_{\|}^2 \quad . \tag{5.7}$$

Because ω_2 is negative, the pc-wave travels in the $-\underset{\sim}{k}_{pc}$ direction if $k_{pc,z}$ is real. In the case of an evanescent pc-wave the wave should die out in the positive z-direction. Consequently, the root should be taken as

$$k_{pc,z} = \begin{cases} -\sqrt{k^2\rho^2 - k_{\|}^2} \quad , & \text{if } k\rho > k_{\|} \quad , \\ \\ i\sqrt{k_{\|}^2 - k^2\rho^2} \quad , & \text{if } k\rho < k_{\|} \quad . \end{cases} \tag{5.8}$$

Then it remains to determine $\underset{\sim}{E}_r$ and $\underset{\sim}{E}_{pc}$.

5.2 Region $0 > z > -\Delta$

Inside the PC the fields are combinations of a- and b-solutions, and we have

$$\underset{\sim}{\hat{E}}(\underset{\sim}{r},\omega_1) = \underset{\sim}{E}_a^+ e^{i\underset{\sim}{k}_a^+\cdot\underset{\sim}{r}} + \underset{\sim}{E}_a^- e^{i\underset{\sim}{k}_a^-\cdot\underset{\sim}{r}} + \eta_b\underset{\sim}{E}_b^+ e^{i\underset{\sim}{k}_b^+\cdot\underset{\sim}{r}} + \eta_b\underset{\sim}{E}_b^- e^{i\underset{\sim}{k}_b^-\cdot\underset{\sim}{r}} \quad , \tag{5.9}$$

$$\underset{\sim}{\hat{E}}(\underset{\sim}{r},\omega_2) = \eta_a\underset{\sim}{E}_a^+ e^{i\underset{\sim}{k}_a^+\cdot\underset{\sim}{r}} + \eta_a\underset{\sim}{E}_a^- e^{i\underset{\sim}{k}_a^-\cdot\underset{\sim}{r}} + \underset{\sim}{E}_b^+ e^{i\underset{\sim}{k}_b^+\cdot\underset{\sim}{r}} + \underset{\sim}{E}_b^- e^{i\underset{\sim}{k}_b^-\cdot\underset{\sim}{r}} \quad . \tag{5.10}$$

The values of k_a^2 and k_b^2 are given in Eq. (3.20), and for the z-components of the wave vectors we write

$$k_{a,z}^{\pm} = \pm k_1 \quad , \tag{5.11}$$

$$k_{b,z}^{\pm} = \pm k_2 \quad , \tag{5.12}$$

with

$$k_1^2 = k_a^2 - k_\parallel^2 \quad , \tag{5.13}$$

$$k_2^2 = k_b^2 - k_\parallel^2 \quad . \tag{5.14}$$

The roots are taken (arbitrarily) as

$$k_1 = \begin{cases} -\sqrt{k_a^2 - k_\parallel^2} \quad , & \text{if } k_a^2 > k_\parallel^2 \quad , \\ -i\sqrt{k_\parallel^2 - k_a^2} \quad , & \text{if } k_a^2 < k_\parallel^2 \quad , \end{cases} \tag{5.15}$$

$$k_2 = \begin{cases} -\sqrt{k_b^2 - k_\parallel^2} \quad , & \text{if } k_b^2 > k_\parallel^2 \quad , \\ i\sqrt{k_\parallel^2 - k_b^2} \quad , & \text{if } k_b^2 < k_\parallel^2 \quad . \end{cases} \tag{5.16}$$

5.3 Region $z < -\Delta$

The only waves which travel or die out in the negative z-direction are

$$\underset{\sim}{\hat{E}}(\underset{\sim}{r},\omega_1) = \underset{\sim}{E}_t \, e^{i\underset{\sim}{k}\cdot\underset{\sim}{r}} \quad , \tag{5.17}$$

$$\underset{\sim}{\hat{E}}(\underset{\sim}{r},\omega_2) = \underset{\sim}{E}_{n\ell} \, e^{i\underset{\sim}{k}_{n\ell}\cdot\underset{\sim}{r}} \quad , \tag{5.18}$$

where the wave vector of the transmitted (t) wave is the same as the incident wave vector. Furthermore, there is possibly a nonlinear ($n\ell$) wave of frequency ω_2, which has

$$k_{n\ell,z} = -k_{pc,z} \quad . \tag{5.19}$$

Figure 2 illustrates the various occurring waves.

6. Polarization and Fresnel coefficients

According to Eq. (5.2) every (complex-valued) wave vector $\underset{\sim}{k}_\alpha$ lies in the plane of incidence, spanned by the (real-valued) vectors $\underset{\sim}{k}_\parallel$ and $\underset{\sim}{e}_z$. The ampliude-polarization vectors $\underset{\sim}{E}_\alpha$ can be decomposed into a surface (s) polarized and a plane (p) polarized component, which are perpendicular to and lie in the plane of incidence, respectively. Since $\underset{\sim}{E}_\alpha$ is restricted by $\underset{\sim}{k}_\alpha \cdot \underset{\sim}{E}_\alpha = 0$, the only ambiguity in a decomposition along unit s- and p-polarization vectors is the choice of the phase of the unit vectors. We take

$$\underset{\sim}{e}_{\alpha s} = \frac{1}{k_\parallel} (\underset{\sim}{k}_\parallel \times \underset{\sim}{e}_z) \quad , \tag{6.1}$$

$$\underset{\sim}{e}_{\alpha p} = \frac{1}{k_\parallel k_\alpha} (k_{\alpha,z} \underset{\sim}{k}_\parallel - k_\parallel^2 \underset{\sim}{e}_z) \quad , \tag{6.2}$$

and it is easy to check that $\underset{\sim}{e}_{\alpha s}$, $\underset{\sim}{e}_{\alpha p}$ and $\underset{\sim}{k}_\alpha / k_\alpha$ constitute an orthornormal set of unit vectors for every α. Notice that $\underset{\sim}{e}_{\alpha s}$ is defined as independent of α and is real. The p-polarization vector can be complex. For all waves only the value of k_α^2 (real) is prescribed by the dispersion relation, and we take the square root as

$$k_\alpha = \begin{cases} \sqrt{k_\alpha^2} \quad , & \text{if } k_\alpha^2 > 0 \quad , \\ i\sqrt{-k_\alpha^2} \quad , & \text{if } k_\alpha^2 < 0 \quad . \end{cases} \tag{6.3}$$

It can be proven that every wave is an s(p)-wave if the incident wave is an s(p)-wave. Therefore, we can distinguish between two cases and write

$$\underset{\sim}{E}_\alpha = E_\alpha \, \underset{\sim}{e}_{\alpha\sigma} \quad , \quad \sigma = s \text{ or } p \quad , \tag{6.4}$$

for every α. The simplification lies in the following relations for the z-components of $\underset{\sim}{E}_\alpha$:

$$\begin{aligned} E_{\alpha,z} &= 0 \quad , \quad s \text{ waves} \quad , \\ E_{\alpha,z} &= -\frac{k_\parallel}{k_\alpha} E_\alpha \quad , \quad p \text{ waves} \quad . \end{aligned} \tag{6.5}$$

Then the Fresnel coefficients $X_\alpha(Y_\alpha)$ for s(p)-waves are defined as the ratio of E_α and E_{inc}, or equivalently the amplitudes $\underset{\sim}{E}_\alpha$ are written as

$$\begin{aligned} \underset{\sim}{E}_\alpha &= X_\alpha \, E_{inc} \, \underset{\sim}{e}_{\alpha s} \quad , \quad \text{for s-waves} \quad , \\ \underset{\sim}{E}_\alpha &= Y_\alpha \, E_{inc} \, \underset{\sim}{e}_{\alpha p} \quad , \quad \text{for p-waves} \quad . \end{aligned} \tag{6.6}$$

The amplitude E_{inc} of the incident field is a given quantity, and the unit polarization vectors $\underset{\sim}{e}_{\alpha\sigma}$ are geometrically determined. Therefore, knowledge of X_α and Y_α for every wave α determines the scattering of any wave by the PC.

7. Solution

Maxwell's equations (2.3) state that at the boundaries $z = 0$ and $z = -\Delta$ the tangential component of $\underset{\sim}{E}$, the normal component of $\underset{\sim}{E} + \underset{\sim}{P}/\epsilon_0$, and the $\underset{\sim}{B}$ field must be continuous, both for ω_1 and ω_2. In matching the fields in the three regions across the boundaries, we can evaluate all $\underset{\sim}{E}_\alpha$'s, and the results

can be expressed in terms of the Fresnel coefficients X_α and Y_α for s- and p-waves, respectively. It is convenient to express the Fresnel coefficients in dimensionless quantities, rather than in wave numbers. Besides ρ and ϵ we introduce

$$u = -k_z/k \quad , \tag{7.1}$$

which allows us to write for the parallel components

$$k_\parallel^2 = k^2(1-u^2) \quad . \tag{7.2}$$

For a travelling incident wave u is real, restricted by $0 \leq u \leq 1$, and u equals the cosine of the angle of incidence. If the incident wave is evanescent, then u is positive imaginary. Furthermore, we define dimensionless wave numbers by

$$m_\alpha = k_\alpha/k \quad , \quad \alpha = a,b,1,2 \quad , \tag{7.3}$$

$$m_p = k_{pc,z}/k \quad , \tag{7.4}$$

and the layer thickness d in units of a wavelength of the incident radiation

$$d = k\Delta/2\pi \quad . \tag{7.5}$$

Due to boundary conditions at $z = -\Delta$, phase factors appear which can be expressed as

$$\psi_1 = -2\pi d m_1 \quad , \quad \psi_2 = 2\pi d m_2 \quad ,$$

(7.6)

$$\psi_3 = 2\pi du \quad . \quad \psi_4 = 2\pi dm_p \quad .$$

For travelling waves these phases are real, and for evanescent waves they are positive imaginary.

After laborous computations, it follows that the Fresnel coefficients can be expressed in terms of eight dimensionless parameters x_i, y_i, $i = 1,\ldots,4$ as follows:

$$X_a^+ = x_1 \quad , \quad X_a^- = x_2 \quad ,$$

$$X_b^+ = x_3 \quad , \quad X_b^- = x_4 \quad ,$$

$$X_r = x_1 + x_2 + \eta_b(x_3+x_4) - 1 \quad ,$$

$$X_{pc} = \eta_a(x_1+x_2) + x_3 + x_4 \quad ,$$

$$X_t = e^{-i\psi_3}\{x_1 e^{i\psi_1} + x_2 e^{-i\psi_1} + \eta_b(x_3 e^{-i\psi_2} + x_4 e^{i\psi_2})\}$$

$$X_{n\ell} = e^{-i\psi_4}\{\eta_a(x_1 e^{i\psi_1} + x_2 e^{-i\psi_1}) + x_3 e^{-i\psi_2} + x_4 e^{i\psi_2}\} \quad ,$$

$$Y_a^+ = m_a y_1 \quad , \quad Y_a^- = m_a y_2 \quad ,$$

$$Y_b^+ = m_b y_3 \quad , \quad Y_b^- = m_b y_4 \quad ,$$

$$Y_r = m_a^2(y_1+y_2) + \eta_b m_b^2(y_3+y_4) - 1 \quad ,$$

$$Y_{pc} = \rho^{-1}\{\eta_a m_a^2(y_1+y_2) + m_b^2(y_3+y_4)\} \quad ,$$

$$Y_t = e^{-i\psi_3}\{m_a^2(y_1 e^{i\psi_1}+y_2 e^{-i\psi_1}) + \eta_b m_b^2(y_3 e^{-i\psi_2}+y_4 e^{i\psi_2})\} \quad ,$$

$$Y_{n\ell} = \rho^{-1}\, e^{-i\psi_4}\{\eta_a m_a^2(y_1 e^{i\psi_1}+y_2 e^{-i\psi_1}) + m_b^2(y_3 e^{-i\psi_2}+y_4 e^{i\psi_2})\} \quad . \qquad (7.7)$$

Here, the parameters x_i and y_i for s- and p-waves, respectively, are solutions of the linear sets

$$P \begin{pmatrix} x_1 \\ x_2 \\ x_3 \\ x_4 \end{pmatrix} = \begin{pmatrix} 2u \\ 0 \\ 0 \\ 0 \end{pmatrix} \quad , \qquad Q \begin{pmatrix} y_1 \\ y_2 \\ y_3 \\ y_4 \end{pmatrix} = \begin{pmatrix} 2u^2 \\ 0 \\ 0 \\ 0 \end{pmatrix} \qquad (7.8)$$

where the matrices P and Q are given by

$$P = \begin{pmatrix} u-m_1 & u+m_1 & \eta_b(u-m_2) & \eta_b(u+m_2) \\ \eta_a(m_p-m_1) & \eta_a(m_p+m_1) & m_p-m_2 & m_p+m_2 \\ -(m_1+u)e^{i\psi_1} & (m_1-u)e^{-i\psi_1} & -\eta_b(m_2+u)e^{-i\psi_2} & \eta_b(m_2-u)e^{i\psi_2} \\ -\eta_a(m_1+m_p)e^{i\psi_1} & \eta_a(m_1-m_p)e^{-i\psi_1} & -(m_2+m_p)e^{-i\psi_2} & (m_2-m_p)e^{i\psi_2} \end{pmatrix}$$

(7.9)

$$Q = \begin{pmatrix} m_1(m_1-u) - (1-u^2)(m_a^2-1) & m_1(m_1+u) - (1-u^2)(m_a^2-1) \\ \eta_a\{m_1(m_1-m_p) - (1-u^2)((m_a/\rho)^2-1)\} & \eta_a\{m_1(m_1+m_p) - (1-u^2)((m_a/\rho)^2-1)\} \\ e^{i\psi_1}\{m_1(m_1+u) - (1-u^2)(m_a^2-1)\} & e^{-i\psi_1}\{m_1(m_1-u) - (1-u^2)(m_a^2-1)\} \\ \eta_a e^{i\psi_1}\{m_1(m_1+m_p) - (1-u^2)((m_a/\rho)^2-1)\} & \eta_a e^{-i\psi_1}\{m_1(m_1-m_p) - (1-u^2)((m_a/\rho)^2-1)\} \end{pmatrix}$$

$$\begin{pmatrix} \eta_b\{m_2(m_2-u) - (1-u^2)(m_b^2-1)\} & \eta_b\{m_2(m_2+u) - (1-u^2)(m_b^2-1)\} \\ m_2(m_2-m_p) - (1-u^2)((m_b/\rho)^2-1) & m_2(m_2+m_p) - (1-u^2)((m_b/\rho)^2-1) \\ \eta_b e^{-i\psi_2}\{m_2(m_2+u) - (1-u^2)(m_b^2-1)\} & \eta_b e^{i\psi_2}\{m_2(m_2-u) - (1-u^2)(m_b^2-1)\} \\ e^{-i\psi_2}\{m_2(m_2+m_p) - (1-u^2)((m_b/\rho)^2-1)\} & e^{i\psi_2}\{m_2(m_2-m_p) - (1-u^2)((m_b/\rho)^2-1)\} \end{pmatrix}. \tag{7.10}$$

The sets of equations from Eq. (7.8) can readily be solved analytically, but the resulting expressions are lengthy and, in turn, not transparent. Numerically, one solves the sets directly, rather than inverting the matrices P and Q.

8. Special case

Although the results of the previous section apply to any situation, in many practical cases the solution can be simplified considerably because of restrictions on the order of magnitude of various parameters. It is elucidating to work out a special limit in order to reveal the fundamental structure of the Fresnel coefficients. If the incident field is a visible narrow-bandwidth laser and exactly on resonance with $\bar{\omega}$, then the relative detuning is of the order of $|\rho-1| \sim 10^{-8}$. Furthermore, the nonlinear coupling

parameter γ_0 has an order of magnitude of 10^{-3} - 10^{-6}, even for very strong CW pump fields. In this section we consider the limit $\gamma_0 \to 0$ (weak interaction) and $\rho \to 1$ (resonance), which implies $\gamma_0 \ll |u^2|$ and $|\rho-1| \ll |u^2|$. First we expand the matrices P and Q up to leading order in ρ - 1 and γ_0, and in the end we take the limits. For this situation the amplitude factors are related by

$$\eta_b = -\eta_a^* \quad , \tag{8.1}$$

and η_a equals

$$\eta_a = -e^{i\phi}\{\frac{1-\rho}{\gamma_0} + \delta\sqrt{1 + (\frac{1-\rho}{\gamma_0})^2}\} \quad , \tag{8.2}$$

which is not necessarily a small parameter. Equation (8.1) expresses that the coupling strength between the two fields of the a-solution equals the coupling strength between the two components of the b-solution. This must be so in this limit, since $\rho \simeq 1$, $\gamma \to 0$ implies $k_a^2 \simeq k_b^2$ and consequently the two branches of the dispersion relation coincide.

8.1 Travelling waves

For $0 \leq u \leq 1$ the incident field is a travelling wave. In lowest order we find for the relative wave numbers

$$m_p = m_1 = m_2 = -u \quad , \tag{8.3}$$

$$m_a = m_b = 1 \quad ,$$

and the Fresnel coefficients are found to be

$$X_a^- = Y_a^- = X_b^- = Y_b^- = X_r = Y_r = X_{n\ell} = Y_{n\ell} = 0 \quad , \tag{8.4}$$

$$X_a^+ = Y_a^+ = \frac{1}{1 + |\eta_a|^2 \, e^{i(\psi_1+\psi_2)}} \quad ,$$

$$X_b^+ = Y_b^+ = \frac{-\eta_a}{e^{-i(\psi_1+\psi_2)} + |\eta_a|^2} \quad ,$$

$$X_t = Y_t = e^{-i(\psi_2+\psi_3)} \frac{1 + |\eta_a|^2}{e^{-i(\psi_1+\psi_2)} + |\eta_a|^2} \quad ,$$

$$X_{pc} = Y_{pc} = \eta_a \frac{e^{-i(\psi_1+\psi_2)} - 1 + |\eta_a|^2(1-e^{i(\psi_1+\psi_2)})}{(1+|\eta_a|^2 e^{i(\psi_1+\psi_2)})(e^{-i(\psi_1+\psi_2)}+|\eta_a|^2)} \quad . \tag{8.5}$$

This limit has several remarkable features. First, the Fresnel coefficients for s- and p-waves are identical, and therefore the scattering process is polarization independent. Second, the specularly-reflected wave disappears, and hence the field which is reflected back into the region $z > 0$ consists entirely of the phase-conjugated signal with respect to the incident beam (times a factor). Third, the structure of X_{pc} is completely determined by phase factors, in the combination

$$\psi_1 + \psi_2 = -2\pi d(m_1 - m_2) \quad . \tag{8.6}$$

According to Eq. (8.3), we have $m_1 - m_2 = 0$ in first order in ρ-1 and γ_0, which would make $\psi_1 + \psi_2 = 0$ and thereby $X_{pc} = 0$. However, $m_1 - m_2$ is multiplied by the relative layer thickness d. For an interaction region of a few centimeters, we have $d \sim 10^5$ and $\psi_1 + \psi_2 \neq 0$, even in lowest order. Since m_1 and m_2 are the relative wave numbers (of the z-component) of the a- and b-waves in the PC, respectively, we conclude that the phase-conjugated signal is brought about by constructive interference between the a- and b-modes of the PC.

If the incident field is in very close resonance with the setting $\bar{\omega}$ of the PC, then we have

$$\eta_a = -\delta e^{i\phi} \quad , \quad |\eta_a| = 1 \quad . \tag{8.7}$$

(More precisely: if $|\rho\text{-}1| \ll \gamma_0$). Under this condition the X_{pc} reduces to

$$X_{pc} = -i\eta_a \tan(\tfrac{1}{2}(\psi_1+\psi_2)) \quad , \tag{8.8}$$

and the PC reflectivity becomes infinite for

$$\psi_1 + \psi_2 = (2n+1)\pi \quad , \quad n \text{ integer} \quad , \tag{8.9}$$

which is the famous resonance condition [3].

Even if $|\rho\text{-}1|$ is not much smaller than γ_0, the denominator of X_{pc}, Eq. (8.5), has still a resonance at the solution of

$$e^{i(\psi_1+\psi_2)} = -1 \quad , \tag{8.10}$$

which leads again to condition (8.9). With θ as the angle of incidence, we then find that the PC is resonant for layer thicknesses

$$d = (n+\tfrac{1}{2}) \frac{\cos\theta}{\sqrt{(1-\rho)^2 + \gamma_0^2}} \quad , \quad n = 0,1,2... \quad . \tag{8.11}$$

At the resonance the value of X_{pc} is found to be

$$X_{pc} = \frac{2\eta_a}{1 - |\eta_a|^2} \quad , \tag{8.12}$$

and in between resonances, where $\exp(i(\psi_1+\psi_2)) = 1$, we have $X_{pc} = 0$. This resonance behavior is illustrated in Fig. 3.

An important conclusion is that when a PC is resonant for radiation under normal incidence ($\theta = 0$), it is off-resonant for radiation which illuminates the surface under a finite angle. In spectroscopic applications, where the incident field is dipole radiation, all plane-wave components strike the PC at a different angle, and therefore, this device cannot operate as a perfect phase conjugator for the entire field.

8.2. Evanescent waves

For an evanescent incident wave we have

$$m_p = -m_1 = m_2 = u \quad , \tag{8.13}$$

and the Fresnel coefficients become

$$X_a^- = X_b^+ = X_r = X_{pc} = 0 \quad ,$$

$$X_a^+ = \frac{1}{1 + |\eta_a|^2} \quad , \quad X_b^- = \frac{-\eta_a}{1 + |\eta_a|^2} \quad ,$$

$$X_t = \frac{e^{-i\psi_3}}{1 + |\eta_a|^2} (e^{i\psi_1} + |\eta_a|^2 e^{i\psi_2}) \quad ,$$

$$X_{n\ell} = \frac{e^{-i\psi_4}}{1 + |\eta_a|^2} \eta_a (e^{i\psi_1} - e^{-i\psi_2}) \quad , \tag{8.14}$$

and the same expressions hold for p-waves. We notice that there is no reflection at all back into the region $z > 0$. Furthermore, if the layer thickness d is much larger than the penetration depth $1/|u|$ of the waves, then the fields in $z < -\Delta$ also vanish. We conclude that there is hardly any reflection of evanescent waves in the limit $\rho \to 1$, $\gamma_0 \to 0$. In Fig. 4 we compare the Fresnel coefficients $|X_{pc}|$ for travelling and evanescent waves. For evanescent waves the nonlinear interaction region is limited to the penetration depth, which is a few optical wavelengths. The PC cannot generate much radiation in such a thin layer, which explains the very small values of X_r and X_{pc} in this case.

9. Resonances

In the previous section we found that $|X_{pc}|$ acquires extreme values if the dimensionless layer thickness d is related to the angle of incidence θ, the detuning ρ and the coupling parameter γ_0 according to Eq. (8.11). These

resonances appear due to perfect phase matching of the a- and b-waves in the PC, as expressed by Eq. (8.10). For $|\rho-1| \ll \gamma_0$ we have $|\eta_a| = 1$, and then $|X_{pc}|$ becomes infinite, as follows from Eq. (8.12). Beside these interference resonances, a PC has a different kind of resonances which appear if we allow the angle of incidence to be nonzero and the waves to become evanescent. If we solve Eq. (7.8) for the eight parameters $x_1,\ldots,x_4$, $y_1,\ldots,y_4$, then the general expression for every parameter is a 3 × 3 determinant (because of the zero's on the right-hand sides), divided by det(P) or det(Q). Resonances then occur for values of ρ, u, γ_0 and d at which det(P) and det(Q) is very small. For instance, in the limit of section 8 we have

$$\det(P) = (2u)^4(e^{-i\psi_2} + |\eta_a|^2 e^{i\psi_1})(e^{-i\psi_1} + |\eta_a|^2 e^{i\psi_2}) \quad , \tag{9.1}$$

for travelling waves, and

$$\det(P) = (2u)^4(1 + |\eta_a|^2)^2 \, e^{-i(\psi_1+\psi_2)} \quad , \tag{9.2}$$

for evanescent waves. Then it is obvious that the right-hand side of Eq. (9.1) has a minimum if the phase-matching condition (8.10) holds, whereas the right-hand side of Eq. (9.2) has no pronounced minima.

Without proof we state that the second kind of resonances can appear there where one of the generated waves turns from a travelling wave into an evanescent wave, or equivalently, at the branch points of the square roots which define the z-components of the wave vectors (section 5). From the expressions of section 5, in combination with relation (7.2) for $k_{\parallel}^2$, we find that the various waves are evanescent under condition:

$$\begin{aligned} \text{r-wave} &: u^2 < 0 \quad , \\ \text{pc-wave} &: u^2 < 1 - \rho^2 \quad , \\ \text{a-waves} &: u^2 < 1 - \epsilon \quad , \\ \text{b-waves} &: u^2 < \epsilon - \rho^2 \quad . \end{aligned} \tag{9.3}$$

Then the resonances are located at $u^2 = 0$, $u^2 = 1 - \rho^2$, $u^2 = 1 - \epsilon$ and $u^2 = \epsilon - \rho^2$. Most obvious is the case $u^2 = 0$, or $u = 0$, for which det(P) must be small according to Eqs. (9.1) and (9.2). We notice that the right-hand sides of (9.3) depend only an γ_0 and ρ, and not on u. For fixed γ_0 and u, the resonances appear at a certain detuning ρ between ω_1 of the incident field and the PC setting frequency $\bar{\omega}$. For γ_0 and ρ fixed we can regard the resonance conditions as an equation for u (angle of incidence or inverse penetration depth) at which $|X_{pc}|$ and the other Fresnel coefficients have sharp peaks. We notice that the positions of the resonances are independent of d, in contrast to the resonances of the previous section.

Let us take ρ and γ_0 fixed, and consider the behavior of the Fresnel coefficients as a function of u. Then the resonances are located at $u = u_{res}$, where the u_{res}'s are solutions of

$$\begin{aligned} \text{pc-wave} &: u_{res}^2 = 1 - \rho^2 \quad , \\ \text{a-waves} &: u_{res}^2 = 1 - \epsilon \quad , \\ \text{b-waves} &: u_{res}^2 = \epsilon - \rho^2 \quad , \end{aligned} \tag{9.4}$$

provided that the equations have a solution in the range of u. We have suppressed the case $u = 0$, since the corresponding extrema are minima. The right-hand sides of Eq. (9.4) are real, and the range of u^2 is $-\infty < u^2 \leq 1$. To see the physical significance of the resonance conditions, we look at

$u_{res}^2 = 1 - \rho^2$ for the pc-wave, and the same picture will hold for the a- and b-waves. If $1 - \rho^2 > 1$ there is no solution, and the Fresnel coefficients will vary smoothly as a function of u. For $0 < 1 - \rho^2 < 1$ there is a solution with $0 < u_{res}^2 < 1$, which implies $0 < u_{res} < 1$ because the u-values are restricted by $0 \leq u \leq 1$, and $u = iv$ with $v > 0$. This situation corresponds to a travelling incident wave with $u = u_{res}$. For $u > u_{res}$ the pc-wave is a travelling wave, and for $u < u_{res}$ the pc-wave is evanescent. Exactly on the transition between the two situations, the Fresnel coefficients have a sharp resonance. In the case that $1 - \rho^2 < 0$ we write $u_{res} = iv_{res}$, and the solution is $v_{res} = (\rho^2-1)^{\frac{1}{2}}$. Then the incident wave is evanescent, and the pc-wave is evanescent for $v > v_{res}$ and travelling for $v < v_{res}$. We notice the remarkable fact that an evanescent incident wave can be reflected by the pc as a travelling wave.

In Figs. 5 and 6 we have plotted $|X_{pc}|$ for a travelling and an evanescent incident field, respectively. Curves a and b correspond to $\omega_1/\bar{\omega} = 1.05$ and $\omega_1/\bar{\omega} = 0.95$, which gives $\rho = 0.905$ and $\rho = 1.105$, respectively. We chose the value 0.05 for parameter γ. Then the solutions of Eq. (9.4) are for curves a

$$\begin{aligned} &\text{pc-wave} \;:\; u = 0.43 \;, \\ &\text{a-waves} \;:\; v = 0.10 \;, \\ &\text{b-waves} \;:\; u = 0.44 \;, \end{aligned} \tag{9.5}$$

and for curves b

$$\begin{aligned} &\text{pc-wave} \;:\; v = 0.47 \;, \\ &\text{a-waves} \;:\; u = 0.11 \;, \\ &\text{b-waves} \;:\; v = 0.48 \;. \end{aligned} \tag{9.6}$$

For a travelling incident wave with $\omega_1 > \bar{\omega}$, there are two resonances as a function of u, and for an evanescent incident wave with $\omega_1 > \bar{\omega}$ there is only a single resonance as a function of v. If $\omega_1 < \bar{\omega}$ there is only one resonance for a travelling incident wave, but two for an evanescent wave. If $\rho \simeq 1$ and $\gamma \simeq 0$ then the two resonances are always very close together. This can be understood from the fact that ϵ is very close to unity in this limit.

10. Specular reflection

Ir the limit of a weak interaction ($\gamma \simeq 0$), in combination with close resonance ($\rho \simeq 1$), the Fresnel coefficients for the specularly-reflected waves at the incident frequency ω_1 are vanishingly small (section 8). For large angles of incident θ, the parameter $u^2 = \cos^2\theta$ (travelling incident wave) can be on the order of γ_0 or $|\rho-1|$, in which case the approximations of section 8 are not accurate. Since the specular wave is also reflected back into the region $z > 0$, it will interfere with the pc-wave, and therefore we cannot neglect this component in the situation of grazing incidence. Figures 7 and 8 illustrate the behavior of $|X_r|$ for various angles of incidence. For $\gamma \simeq 0$ and $u \simeq 1$, $|X_r|$ indeed disappears, but for $u \to 0$ the value of $|X_r|$ approaches unity. Phase matching between the a- and b-waves in the PC is again responsible for the oscillatory behavior of $|X_r|$ as a function of d.

11. Conclusions

We have studied the scattering of travelling and evanescent waves by a phase conjugator in the four-wave mixing configuration, without restrictions on the angle of incidence, the interaction strength or the frequency detuning with the pump beams. The Fresnel coefficients for the various waves were derived from Maxwell's equations, subject to the appropriate boundary conditions,

without the usual slowly-varying amplitude approximation. It was shown that in the limit of weak coupling and perfect resonance, the reflection coefficient for the pc-wave reduces to the well-known result (8.8), which implies the resonance condition (8.9) for a four-wave mixing PC. We were able to track down the origin of these resonances to perfect phase matching between the two (a and b) modes of the PC. In addition, we found strong resonances at these values of the parameters where one of the waves (a, b or pc) turns from a travelling wave into an evanescent wave. We were not able to find a convincing physical explanation for these resonances, but from numerical examples it follows that they are definitely present. Finally, we showed that for large angles of incidence the nonlinear specularly-reflected wave has an amplitude of the same order as the pc-wave.

Acknowledgments

This research was supported by the Air Force Office of Scientific Research (AFSC), United States Air Force, under Contract F49620-86-0009, and the Office of Naval Research. The United States Government is authorized to reproduce and distribute reprints for governmental purposes, notwithstanding any copyright notation hereon.

References

[1] Pepper, D. M., 1982, Opt. Eng., 21, 156.

[2] Fisher, R. A., editor, 1983, Optical Phase Conjugation (New York: Academic).

[3] Zel'dovich, B. Ya., Pilipetskii, N. F., and Shkunov, V. V., 1985, Principles of Phase Conjugation (Berlin : Springer).

[4] Pepper, D. M., Fekete, D., and Yariv, A., 1978, Appl. Phys. Lett., 33, 41.

[5] Feinberg, J., 1983, Opt. Lett., 8, 480.

[6] Salamo, G., Miller, M. J., Clark III, W. W., Wood, G. L., and Sharp, E. J., 1986, Opt. Commun., 59, 417.

[7] Lindsay, I., and Dainty, J. C., 1986, Opt. Commun., 59, 405.

[8] Jacobs, A. A., Tompkin, W. R., Boyd, R. W., and Wolf, E., 1987, J. Opt. Soc. Am. B 4, 1266.

[9] Kurokawa, K., Hattori, T., and Kobayashi, T., 1987, Phys. Rev. A, 36, 1298.

[10] Yariv, A., 1978, IEEE J. of Quant. Electr., QE-14, 650.

[11] Fisher, R. A., Suydam, B. R., and Feldman, B. J., 1981, Phys. Rev. A, 23, 3071.

[12] Suydam, B. R., and Fisher, R.A., 1982, Opt. Eng., 21, 184.

[13] Friberg, A. T., and Drummond, P. D., 1983, J. Opt. Soc. Am., 73, 1216.

[14] Suydam, B. R., 1983, J.Opt. Soc. Am., 73, 539.

[15] Reiner, G., Meystre, P., and Wright, E. M., 1987, J. Opt. Soc. Am. B, 4, 675.

[16] An, S., Capron, B. A., and Sargent III, M., 1987, Opt. Commun., 64, 307.

[17] Wolf, E., Mandel, L., Boyd, R. W., Habashy, T. M., and Nieto-Vesperinas, M., 1987, J. Opt. Soc. Am. B, 4, 1260.

[18] Agarwal, G. S., 1987, J. Opt. Soc. Am. B, 4, 1806.

[19] Petersen, P. M., and Johansen, P. M., 1988, Opt. Lett., 13, 45.

[20] Agarwal, G. S., 1982, Opt. Commun., 42, 205.

[21] Bochove, E. J., 1987, Phys. Rev. Lett., 59, 2547.

[22] According to Fourier's theorem, every field can be expanded in terms of travelling plane waves. Maxwell's equations, however, impose the restriction that the field must be transverse. Even when a radiation field is transverse, its Fourier expansion can acquire longitudinal components which do not obey Maxwell's equations individually. This complication can be avoided by allowing the field to consist of travelling and evanescent transverse plane waves.

[23] Arnoldus, H. F., and George, T. F., J. Opt. Soc. Am. B, submitted.

[24] Shen, Y. R., 1984, The Principles of Nonlinear Optics (New York : Wiley).

Figure captions

Figure 1. Dispersion relation for a phase conjugator. Curves a and b are k_a^2/k^2 and k_b^2/k^2, respectively, as a function of $\omega_1/\bar{\omega}$, and the coupling parameter is $\gamma_0 = 0.2$. The discontinuous behavior around $\omega_1 = \bar{\omega}$ comes from the choice of the roots in the definition of η_a and η_b.

Figure 2. Schematic representation of the various waves from section 5. The arrows indicate the wave vectors, which all have the same parallel component $\underline{k}_\parallel$. Their perpendicular components are approximately the same, apart from the sign. The inc-, t- are r-waves are ω_1-waves and they travel in the direction of the wave vector. The pc- and nℓ-waves have a frequency $\omega_2 < 0$, and therefore they travel in the direction opposite to the wave vector. This is indicated by a circle on the arrows. Inside the PC we have four different wave vectors and every vector corresponds to two fields according to Eqs. (5.9) and (5.10). The a+ and a- fields are essentially ω_1-fields, and the b+ and b- fields are negative-frequency waves. For $\gamma \neq 0$ these principle waves couple to a field with the same wave vector but with a frequency of opposite sign. These fields are indicated by broken arrows. The wave which couples to the principle wave always propagates in the opposite direction.

Figure 3. Absolute value of the reflection coefficient for the pc-wave with s-polarization for $u = 1$ and $\gamma = 0.05$, as a function of the layer thickness d. Curves a, b, c and d correspond to $\omega_1/\bar{\omega} = 1.006$, 1.01, 1.05 and 1.1, respectively. The peaks result from interference between a- and b-waves, and the positions of the peaks are given by Eq. (8.11). For larger detunings the peaks shift and become less pronounced, in agreement with Eq. (8.12). In the limit $\omega_1 = \bar{\omega}$, curve a turns into an extremely sharp resonance.

Figure 4. Reflectivity for the phase-conjugated wave as a function of d. The parameters are $\gamma_0 = 0.05$ and $\omega_1/\bar{\omega} = 1.01$. Plot a corresponds to a travelling incident wave ($u = 0.25$), and curve b represents an evanescent field ($u = 0.25i$). The sharp resonances in curve a originate again from phase interference, and their position is given by Eq. (8.11). It is seen that the reflectivity for an evanescent wave is almost negligible, as compared to a travelling wave.

Figure 5. Absolute value of X_{pc} as a function of u for $\gamma = 0.05$, $d = 5$ and $\omega_1/\bar{\omega} = 1.05$ (curve a) and $\omega_1/\bar{\omega} = 0.95$ (curve b). The two peaks in curve a are situated at $u_{res} = 0.43$ and $u_{res} = 0.44$, and they appear because the pc-wave and the b-wave become evanescent for lower values of u. In curve b the left-most peak corresponds to an evanescent a-wave for lower values of u, and the other peak is a phase-matching interference from section 8.

Figure 6. Same as Fig. 5, but now as a function of $v = -iu$. For v larger than the resonance of curve a the a-wave is evanescent, and for v larger than 0.48, both the pc-wave and the b-wave are evanescent, which gives rise to the peaks in curve b.

Figure 7. Reflection coefficient for the specular wave as a function of the normalized layer thickness d. The parameters are $\omega_1/\bar{\omega} = 1.01$ and $\gamma = 0.05$. For curves a, b and c we took $u = 0.2$, 0.25 and 0.45, respectively. It is seen that $|X_r|$ is not small for large angles of incidence.

Figure 8. Same as Fig. 7 but with $u = 0.01$ and 0.1 for curves a and b, respectively. In the limit $u \to 0$, $|X_r|$ approaches unity, except at the sharp

valleys, which corresond to a perfect phase mismatch between the a- and b-waves.

Arnoldus and George, fig. 1.

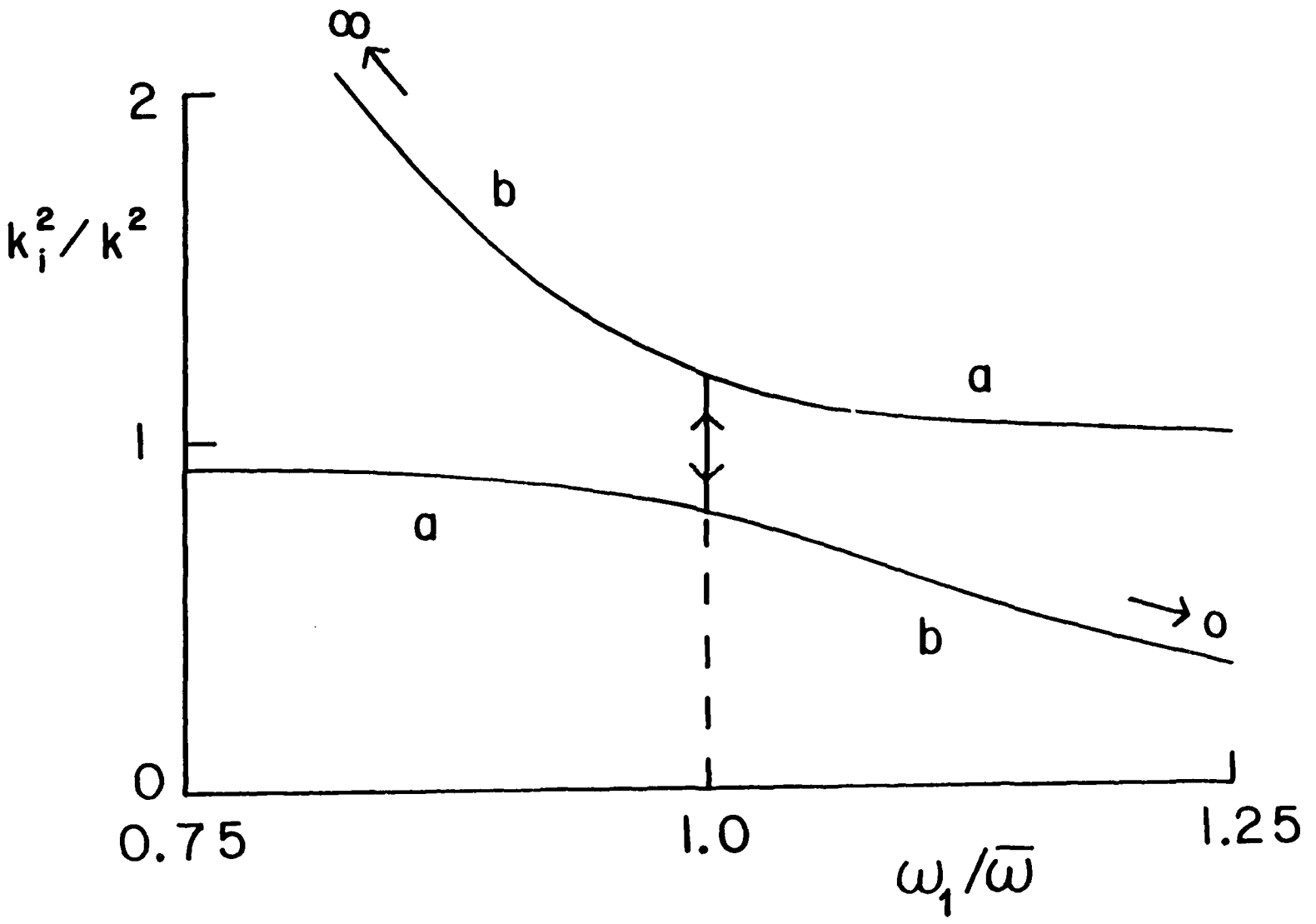

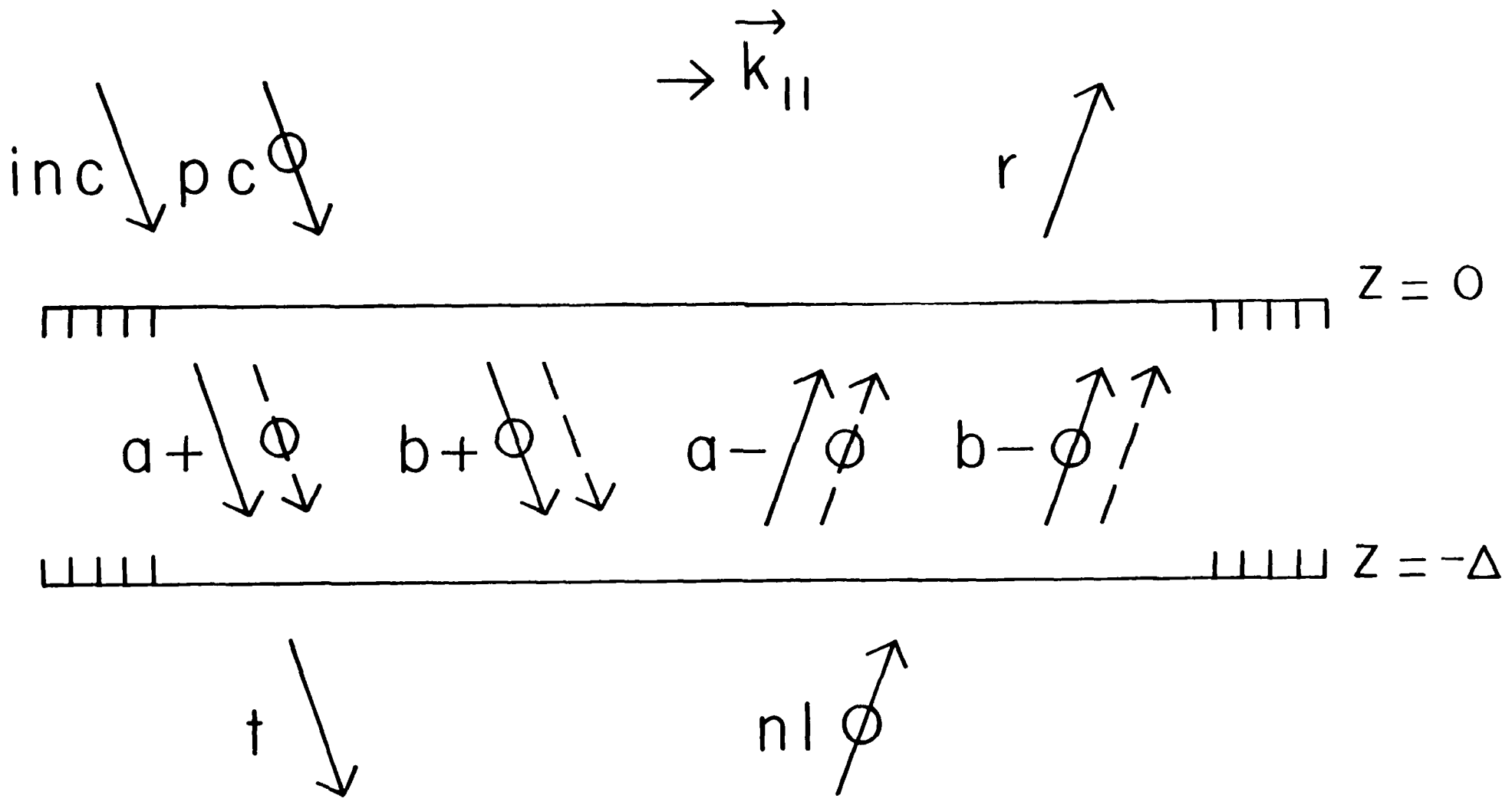
$\rightarrow \vec{k}_{\parallel}$
inc
pc
r
z = 0
a+
b+
a−
b−
z = −Δ
t
nl

Arnoldus and George, fig. 5.

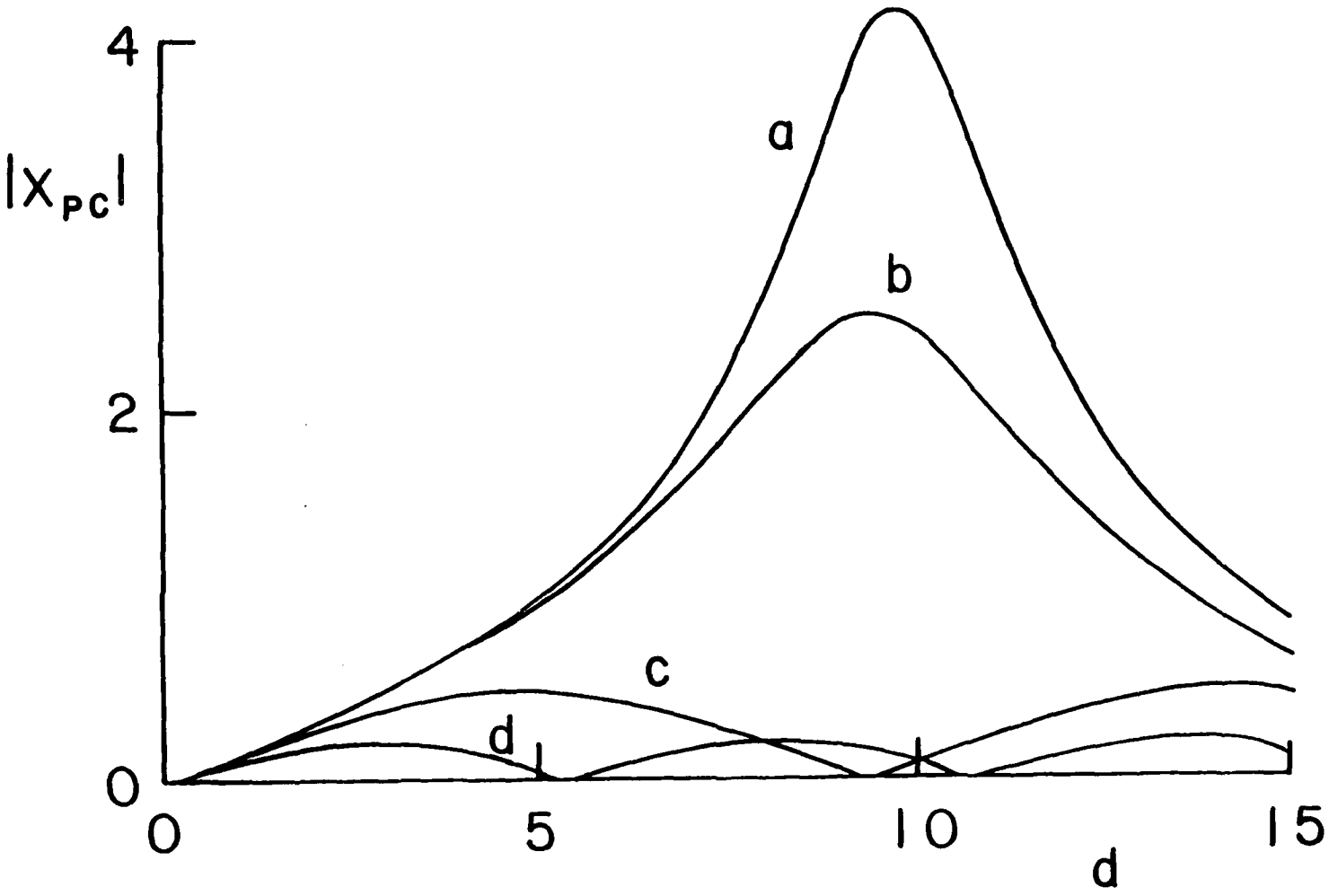

Arnoldus and George, Fig. 4.

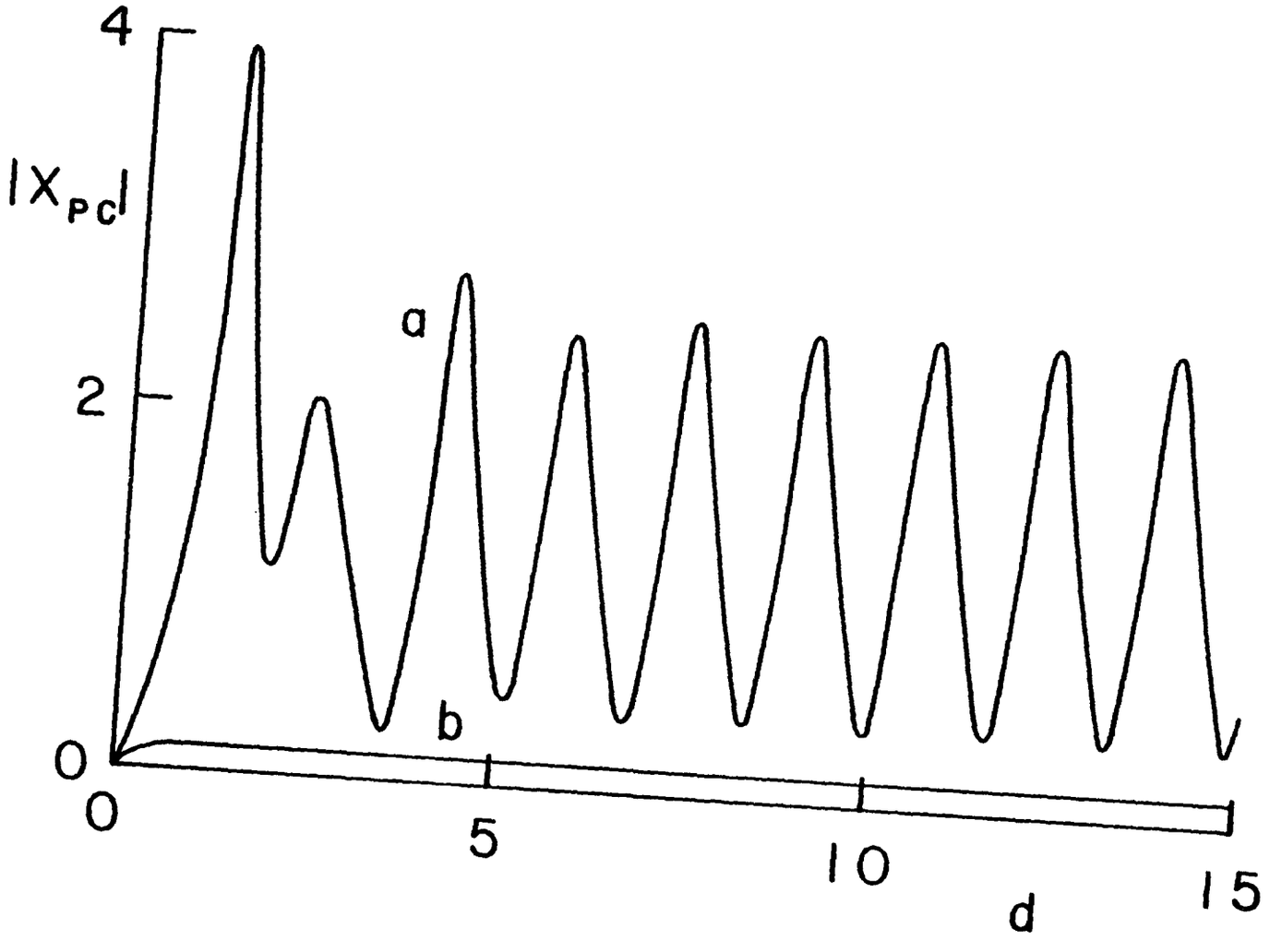

Arnoldus and George, fig. 5

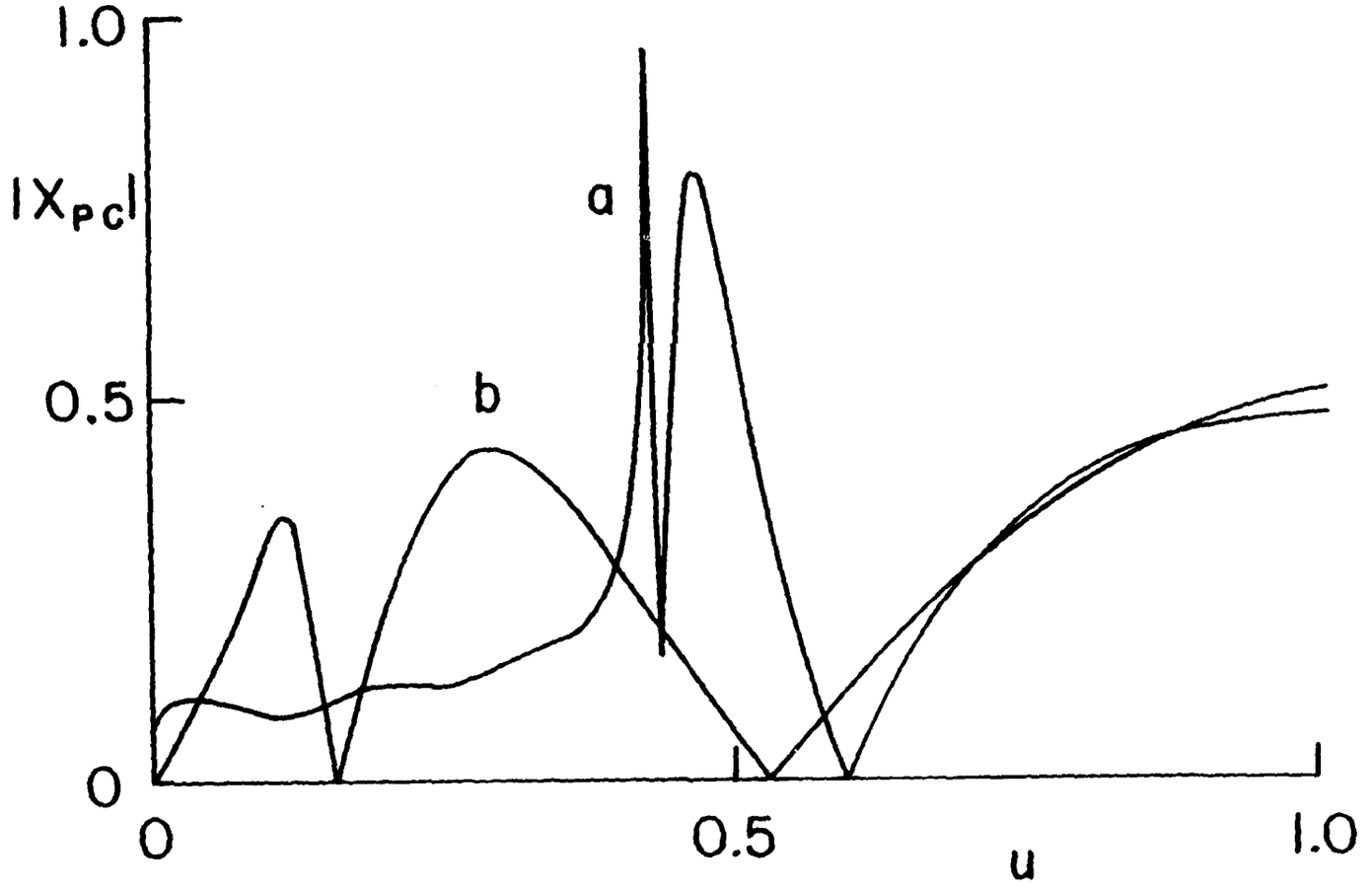

Arnoldus and George, fig. 6.

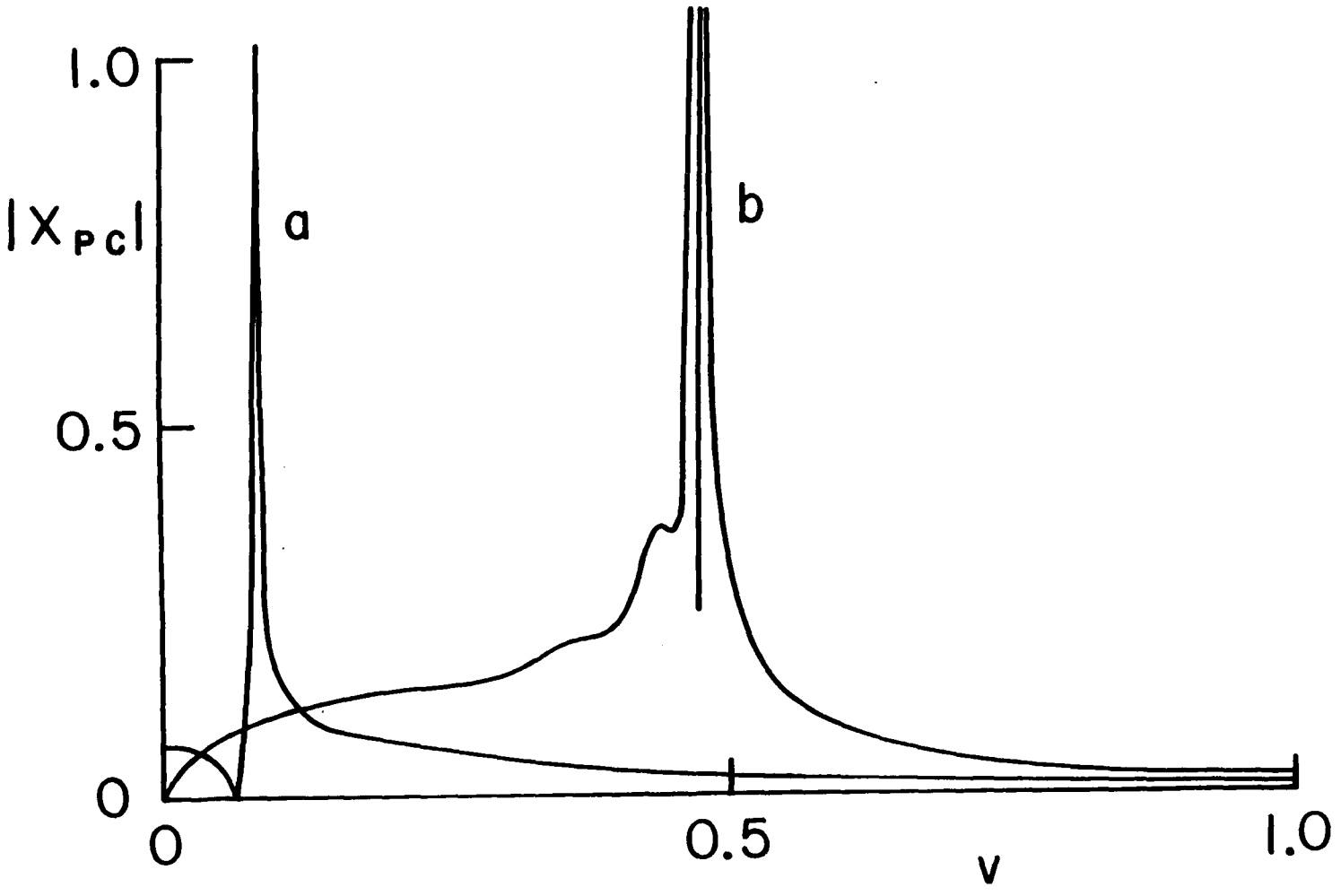

Arnoldus and George, fig. 1.

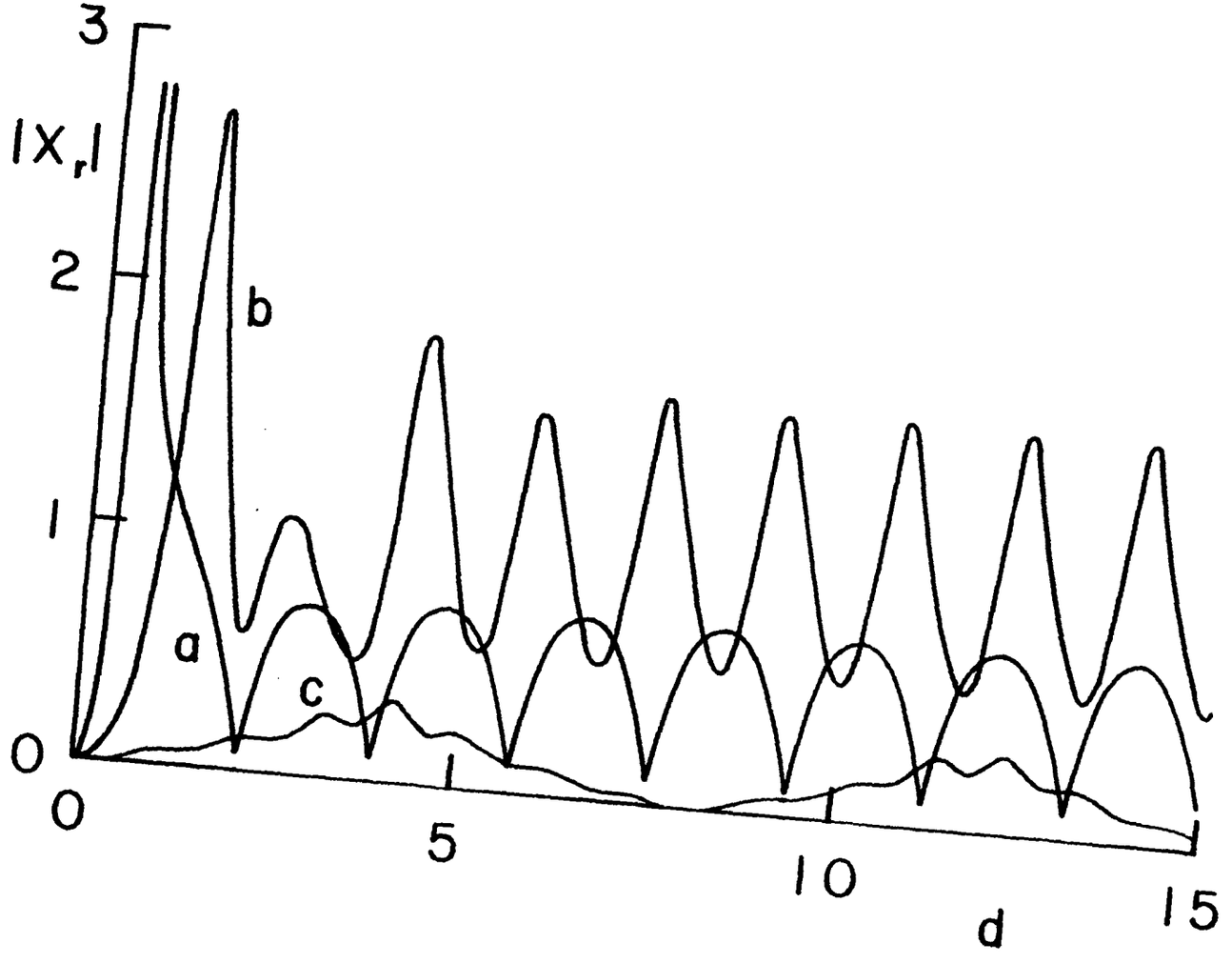

Arnoldus and George, Fig. 8.

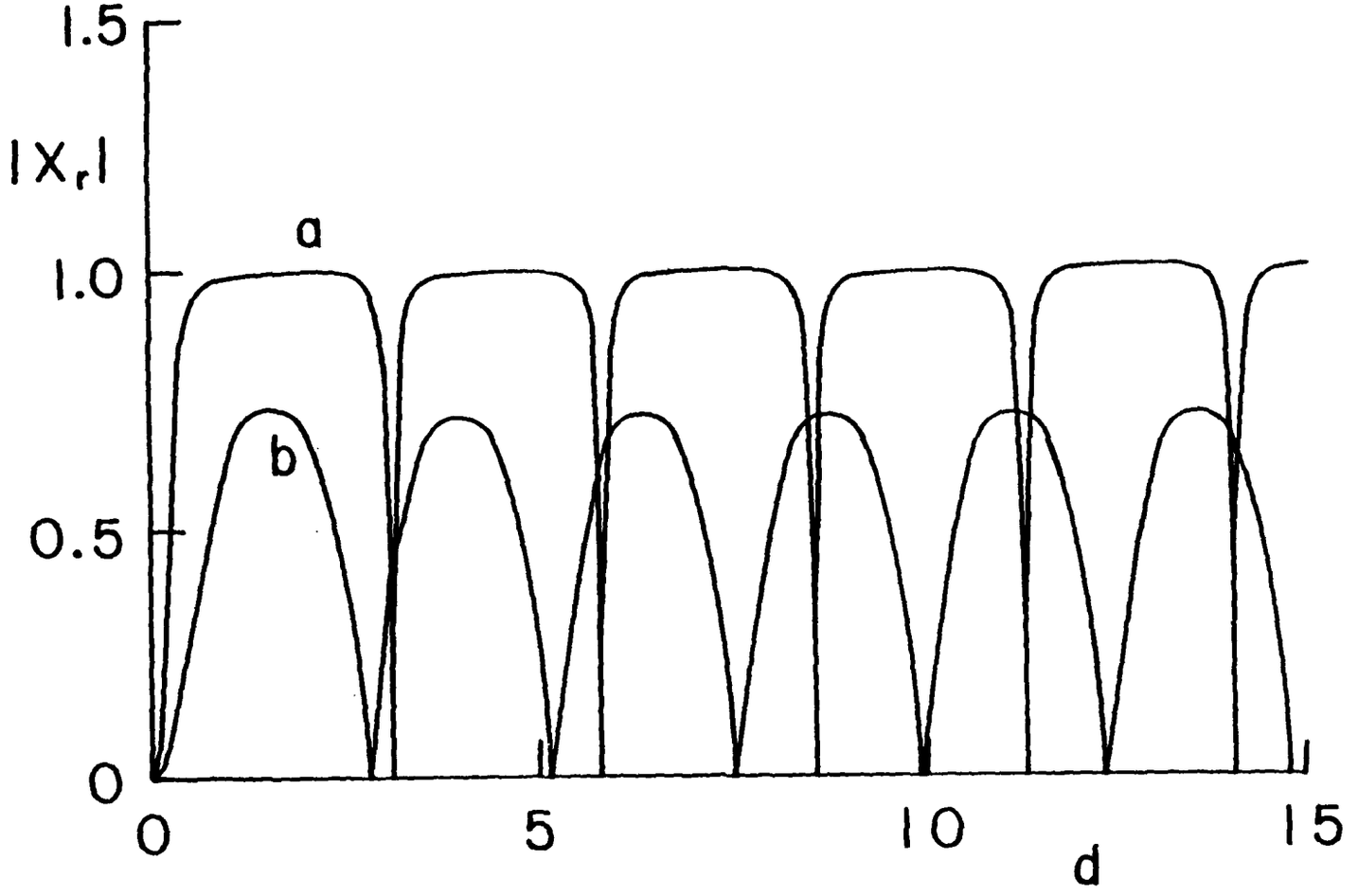

OL/1113/86/2

TECHNICAL REPORT DISTRIBUTION LIST, GEN

	No. Copies
Office of Naval Research Attn: Code 1113 800 N. Quincy Street Arlington, Virginia 22217-5000	2
Dr. Bernard Douda Naval Weapons Support Center Code 50C Crane, Indiana 47522-5050	1
Naval Civil Engineering Laboratory Attn: Dr. R. W. Drisko, Code L52 Port Hueneme, California 93401	1
Defense Technical Information Center Building 5, Cameron Station Alexandria, Virginia 22314	12 high quality
DTNSRDC Attn: Dr. H. Singerman Applied Chemistry Division Annapolis, Maryland 21401	1
Dr. William Tolles Superintendent Chemistry Division, Code 6100 Naval Research Laboratory Washington, D.C. 20375-5000	1
Dr. David Young Code 334 NORDA NSTL, Mississippi 39529	1
Naval Weapons Center Attn: Dr. Ron Atkins Chemistry Division China Lake, California 93555	1
Scientific Advisor Commandant of the Marine Corps Code RD-1 Washington, D.C. 20380	1
U.S. Army Research Office Attn: CRD-AA-IP P.O. Box 12211 Research Triangle Park, NC 27709	1
Mr. John Boyle Materials Branch Naval Ship Engineering Center Philadelphia, Pennsylvania 19112	1
Naval Ocean Systems Center Attn: Dr. S. Yamamoto Marine Sciences Division San Diego, California 91232	1
Dr. David L. Nelson Chemistry Division Office of Naval Research 800 North Quincy Street Arlington, Virginia 22217	1

ABSTRACTS DISTRIBUTION LIST, 056/625/629

Dr. J. E. Jensen
Hughes Research Laboratory
3011 Malibu Canyon Road
Malibu, California 90265

Dr. J. H. Weaver
Department of Chemical Engineering
and Materials Science
University of Minnesota
Minneapolis, Minnesota 55455

Dr. A. Reisman
Microelectronics Center of North Carolina
Research Triangle Park, North Carolina
27709

Dr. M. Grunze
Laboratory for Surface Science and
Technology
University of Maine
Orono, Maine 04469

Dr. J. Butler
Naval Research Laboratory
Code 6115
Washington D.C. 20375-5000

Dr. L. Interante
Chemistry Department
Rensselaer Polytechnic Institute
Troy, New York 12181

Dr. Irvin Heard
Chemistry and Physics Department
Lincoln University
Lincoln University, Pennsylvania 19352

Dr. K.J. Klaubunde
Department of Chemistry
Kansas State University
Manhattan, Kansas 66506

Dr. C. B. Harris
Department of Chemistry
University of California
Berkeley, California 94720

Dr. F. Kutzler
Department of Chemistry
Box 5055
Tennessee Technological University
Cookesville, Tennessee 38501

Dr. D. DiLella
Chemistry Department
George Washington University
Washington D.C. 20052

Dr. R. Reeves
Chemistry Department
Renssaeler Polytechnic Institute
Troy, New York 12181

Dr. Steven M. George
Stanford University
Department of Chemistry
Stanford, CA 94305

Dr. Mark Johnson
Yale University
Department of Chemistry
New Haven, CT 06511-8118

Dr. W. Knauer
Hughes Research Laboratory
3011 Malibu Canyon Road
Malibu, California 90265

ABSTRACTS DISTRIBUTION LIST, 056/625/629

Dr. G. A. Somorjai
Department of Chemistry
University of California
Berkeley, California 94720

Dr. J. Murday
Naval Research Laboratory
Code 6170
Washington, D.C. 20375-5000

Dr. J. B. Hudson
Materials Division
Rensselaer Polytechnic Institute
Troy, New York 12181

Dr. Theodore E. Madey
Surface Chemistry Section
Department of Commerce
National Bureau of Standards
Washington, D.C. 20234

Dr. J. E. Demuth
IBM Corporation
Thomas J. Watson Research Center
P.O. Box 218
Yorktown Heights, New York 10598

Dr. M. G. Lagally
Department of Metallurgical
and Mining Engineering
University of Wisconsin
Madison, Wisconsin 53706

Dr. R. P. Van Duyne
Chemistry Department
Northwestern University
Evanston, Illinois 60637

Dr. J. M. White
Department of Chemistry
University of Texas
Austin, Texas 78712

Dr. D. E. Harrison
Department of Physics
Naval Postgraduate School
Monterey, California 93940

Dr. R. L. Park
Director, Center of Materials
Research
University of Maryland
College Park, Maryland 20742

Dr. W. T. Peria
Electrical Engineering Department
University of Minnesota
Minneapolis, Minnesota 55455

Dr. Keith H. Johnson
Department of Metallurgy and
Materials Science
Massachusetts Institute of Technology
Cambridge, Massachusetts 02139

Dr. S. Sibener
Department of Chemistry
James Franck Institute
5640 Ellis Avenue
Chicago, Illinois 60637

Dr. Arnold Green
Quantum Surface Dynamics Branch
Code 3817
Naval Weapons Center
China Lake, California 93555

Dr. A. Wold
Department of Chemistry
Brown University
Providence, Rhode Island 02912

Dr. S. L. Bernasek
Department of Chemistry
Princeton University
Princeton, New Jersey 08544

Dr. W. Kohn
Department of Physics
University of California, San Diego
La Jolla, California 92037

ABSTRACTS DISTRIBUTION LIST, 056/625/629

Dr. F. Carter
Code 6170
Naval Research Laboratory
Washington, D.C. 20375-5000

Dr. Richard Colton
Code 6170
Naval Research Laboratory
Washington, D.C. 20375-5000

Dr. Dan Pierce
National Bureau of Standards
Optical Physics Division
Washington, D.C. 20234

Dr. R. Stanley Williams
Department of Chemistry
University of California
Los Angeles, California 90024

Dr. R. P. Messmer
Materials Characterization Lab.
General Electric Company
Schenectady, New York 22217

Dr. Robert Gomer
Department of Chemistry
James Franck Institute
5640 Ellis Avenue
Chicago, Illinois 60637

Dr. Ronald Lee
R301
Naval Surface Weapons Center
White Oak
Silver Spring, Maryland 20910

Dr. Paul Schoen
Code 6190
Naval Research Laboratory
Washington, D.C. 20375-5000

Dr. John T. Yates
Department of Chemistry
University of Pittsburgh
Pittsburgh, Pennsylvania 15260

Dr. Richard Greene
Code 5230
Naval Research Laboratory
Washington, D.C. 20375-5000

Dr. L. Kesmodel
Department of Physics
Indiana University
Bloomington, Indiana 47403

Dr. K. C. Janda
University of Pittsburg
Chemistry Building
Pittsburg, PA 15260

Dr. E. A. Irene
Department of Chemistry
University of North Carolina
Chapel Hill, North Carolina 27514

Dr. Adam Heller
Bell Laboratories
Murray Hill, New Jersey 07974

Dr. Martin Fleischmann
Department of Chemistry
University of Southampton
Southampton 509 5NH
UNITED KINGDOM

Dr. H. Tachikawa
Chemistry Department
Jackson State University
Jackson, Mississippi 39217

Dr. John W. Wilkins
Cornell University
Laboratory of Atomic and
Solid State Physics
Ithaca, New York 14853

ABSTRACTS DISTRIBUTION LIST, 056/625/629

Dr. R. G. Wallis
Department of Physics
University of California
Irvine, California 92664

Dr. D. Ramaker
Chemistry Department
George Washington University
Washington, D.C. 20052

Dr. J. C. Hemminger
Chemistry Department
University of California
Irvine, California 92717

Dr. T. F. George
Chemistry Department
University of Rochester
Rochester, New York 14627

Dr. G. Rubloff
IBM
Thomas J. Watson Research Center
P.O. Box 218
Yorktown Heights, New York 10598

Dr. Horia Metiu
Chemistry Department
University of California
Santa Barbara, California 93106

Dr. W. Goddard
Department of Chemistry and Chemical Engineering
California Institute of Technology
Pasadena, California 91125

Dr. P. Hansma
Department of Physics
University of California
Santa Barbara, California 93106

Dr. J. Baldeschwieler
Department of Chemistry and Chemical Engineering
California Institute of Technology
Pasadena, California 91125

Dr. J. T. Keiser
Department of Chemistry
University of Richmond
Richmond, Virginia 23173

Dr. R. W. Plummer
Department of Physics
University of Pennsylvania
Philadelphia, Pennsylvania 19104

Dr. E. Yeager
Department of Chemistry
Case Western Reserve University
Cleveland, Ohio 41106

Dr. N. Winograd
Department of Chemistry
Pennsylvania State University
University Park, Pennsylvania 16802

Dr. Roald Hoffmann
Department of Chemistry
Cornell University
Ithaca, New York 14853

Dr. A. Steckl
Department of Electrical and Systems Engineering
Rensselaer Polytechnic Institute
Troy, NewYork 12181

Dr. G.H. Morrison
Department of Chemistry
Cornell University
Ithaca, New York 14853